Environment Canada

Water Science and Technology Directorate

Direction générale des sciences et de la technologie, eau

Environnement Canada

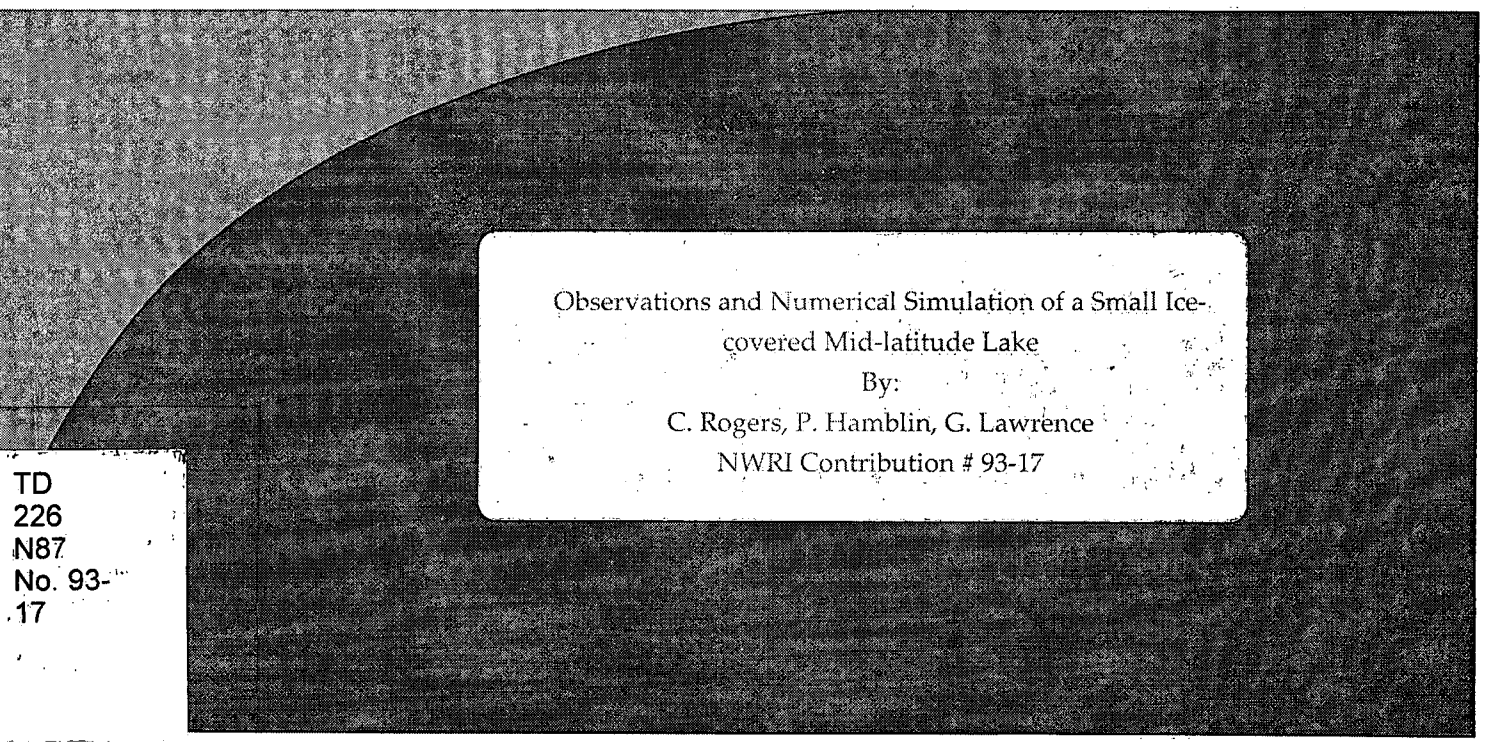

Observations and Numerical Simulation of a Small Ice-covered Mid-latitude Lake

By:

C. Rogers, P. Hamblin, G. Lawrence

NWRI Contribution # 93-17

-17

OBSERVATIONS AND NUMERICAL SIMULATION OF A SMALL ICE-COVERED MID-LATITUDE LAKE

(Running head: Ice-covered lake model)

by

Christopher K. Rogers [1]

Paul F. Hamblin [2]

Gregory A. Lawrence [1]

1. Department of Civil Engineering, University of British Columbia, Vancouver, B.C., Canada. V6T 1Z4.

2. Lakes Research Branch, National Water Research Institute, Burlington, Ontario, Canada. L7R 4A6.

March 2, 1993

Abstract

An existing heat transfer algorithm is extended to permit the simulation of ice and snow cover on a small mid-latitude lake. New features include: snowmelt due to rain, sediment heat transfer, snow-ice formation, and variability in snow density, snow conductivity and albedo. Since the lake considered is nearly isothermal in winter, the new model ignores internal thermodynamics. All discrepancies between field observations and model predictions are accounted for by parameter uncertainties and expected observation error. It was found that sediment heat transfer may be important in early winter in preventing a net loss of heat from the lake water. Significant heat gains in the latter part of winter, however, are attributed to the penetration of solar radiation through the ice.

Acknowledgments

Support for this study was provided by the Natural Sciences and Engineering Research Council (N.S.E.R.C), the Science Council of British Columbia, the University of British Columbia, and the B.C. Ministry of the Environment.

Management Perspective

The study was conducted by a graduate student at the University of British Columbia under the direction of G.A.Lawrence and P.F.Hamblin and the financial support of B.C. Environment and the Natural Sciences and Engineering Research Council of Canada. The study was motivated by the need to ameliorate or eliminate winter fishkill in small interior lakes in British Columbia. While the study comprises an extensive field observational component, a laboratory modelling phase and a mathematical modelling contribution this paper deals primarily with the field observations and mathematical modelling of the control lake located on the southern interior plateau.

Unlike the earlier data collected by Hamblin and Carmack in northern lakes the winter conditions were much more moderate requiring for the first time to take into account rainfall effects on the snow and ice cover and the formation of snow-ice caused by flooding by snow loads and periodic thaws.

It is expected that the effect of a mechanical stirrer on the winter thermal regime and water quality of a nearby treated lake will be reported subsequently.

Introduction

A number of water quality simulation models have been developed to address the need to manage the quality of water stored in lakes and reservoirs. Most are fashioned after the WRE (Water Resources Engineers) model originally developed by Chen and Orlob (1975). Thermal stratification is of primary importance to water quality and therefore much effort has been focused on its prediction. As temperature variations in small to medium sized lakes and reservoirs are for most purposes, only significant in the vertical direction, the one-dimensional horizontal slab concept first advanced by Raphael (1962) is basic to most of these models. The heat budgets of most lakes with high retention times are basically a function of meteorological forcing. For simplicity, bulk aerodynamic formulae, such as those given by the Tennessee Valley Authority (TVA, 1972) are generally applied.

In spite of the existence of many one-dimensional thermodynamic lake models, however, few have tackled the ice-cover problem. Those that have are highly simplified and/or do not deal with some of the important components of the heat budgets of mid-latitude lakes. The current study stems from the need to quantify the thermal impact of artificially creating ice-free areas to allow re-aeration in mid-latitude lakes which would otherwise experience winter fish mortalities. For this investigation, an existing ice and snow-cover model was selected and extended to account for the particular problems associated with ice cover on a small undisturbed lake located in southern British Columbia. This lake is considered to be representative of the winter climatology of temperate zone lakes.

The development of the extended model is presented, followed by a description of the field study at the selected lake, and an analysis of the simulation results.

Model Selection

Gosink (1987) and Patterson & Hamblin (1988) have developed thermodynamic models of ice-covered lakes. Both models use an ice-cover algorithm and integrate it with DYRESM, a commercially available model which has been thoroughly tested and proven for temperate climates (see Imberger & Patterson, 1981). They are also similar in that they use a steady state solution to the heat conduction equation that includes a depth dependent heat source to account for the penetration of solar radiation through the ice and snow. Both models, however, were developed for lakes at high latitude, and have been insufficiently tested on mid-latitude lakes. The Patterson & Hamblin (1988) model is more general than the Gosink (1987) model. In the latter model, no allowance is made for partial ice cover, and the short wave radiation is assumed to consist of only one spectral band characterized by a single attenuation coefficient for each medium through which it passes. Patterson & Hamblin (1988) provide a more accurate representation by dividing the shortwave radiation into its visible and infrared components and assigning different absorption coefficients for each component. Consequently, the Patterson & Hamblin (1988) model, called DYRESMI, was selected and modified for the present study.

A full description of the development of DYRESMI is given in Patterson & Hamblin (1988). Briefly, it is based on the thermodynamic sea ice model proposed by Maykut & Untersteiner (1971). Patterson & Hamblin developed two main improvements to this model. First, a thermodynamic link with the underlying water column as modeled by DYRESM was established, negating the need to specify the heat flux between the water and the ice as an external parameter. Secondly, the effect of partial ice cover was incorporated into the model.

The DYRESMI model has been extended in this study to address the issues which may be of particular concern for mid-latitude lakes. These include rainfall, albedo and snow density variability, and snow-ice formation. In addition, sediment heat transfer, which is of importance in small and shallow lakes, is incorporated into the model.

Theoretical Development

The consideration of snow-ice as a distinct layer in the ice and snow cover, having intermediate properties between snow and ice, requires a re-evaluation of the governing heat conduction equations. Snow-ice forms when the weight of ice and newly fallen snow exceeds the buoyancy of the ice cover. The ice will crack and water will seep into the snow cover. When the water freezes, snow-ice is produced. Therefore the steady state heat conduction equations developed by Patterson & Hamblin (1988) for the proportioning of the short wave radiation into two spectral bands must be extended to include snow-ice as a third component in the cover:

$$K_s \frac{\partial^2 T_s}{\partial z^2} + A_1 \lambda_{s1} I_o \exp[-\lambda_{s1} (h_i+h_e+h_s-z)] + A_2 \lambda_{s2} I_o \exp[-\lambda_{s2} (h_i+h_e+h_s-z)] + Q_{si} = 0,$$
$$h_i + h_e + h_s \geq z \geq h_i + h_e$$

$$K_e \frac{\partial^2 T_e}{\partial z^2} + A_1 \lambda_{e1} I_o \exp[-\lambda_{s1} h_s - \lambda_{e1}(h_i+h_e-z)] + A_2 \lambda_{e2} I_o \exp[-\lambda_{s2} h_s - \lambda_{e2}(h_i+h_e-z)] = 0,$$
$$h_i + h_e \geq z \geq h_i$$

$$K_i \frac{\partial^2 T_i}{\partial z^2} + A_1 \lambda_{i1} I_o \exp[\lambda_{s1} h_s - \lambda_{e1} h_e - \lambda_{i1}(h_i-z)] + A_2 \lambda_{i2} I_o \exp[-\lambda_{s2} h_s - \lambda_{e2} h_e - \lambda_{i2}(h_i-z)] = 0,$$
$$h_i \geq z \geq 0, \qquad (1)$$

where, I_o = incident (non-reflected) radiation
= $(1 - \alpha) \cdot Q_o$, where α = albedo; Q_o = total incoming radiation

I_z = radiation remaining at depth z below the surface

λ = attenuation coefficient

A_1, A_2 = fraction of total radiation in the visible and infrared spectral bands respectively. $A_1 = 0.7$ and $A_2 = 0.3$ in accordance with Kirk (1983) and Boer (1980)

T = material temperature

K = material conductivity

λ = attenuation coefficient

h = material thickness

s = snow

i = ice

e = snow-ice

o = surface

subscripts 1 and 2 refer to the visible and infrared spectral bands, respectively.

The heat source, Q_{si}, accounts for the heat supplied by lake water flooding the snow cover following a heavy snowfall. This source of heat, which is assumed to be distributed over the entire snow thickness, includes the sensible heat given up to the snow layer as it cools to the freezing mark, and the latent heat which is produced when this water freezes to form snow-ice. Although it might be more appropriate to add a fourth medium to the lake cover to reflect that this heat is not distributed over the entire snow thickness, the improvement in results is unlikely to be sufficient to justify further extension of the model.

The appropriate boundary conditions for equation (1) are:

$$T_i = T_f \qquad z = 0$$

$$\left.\begin{aligned} T_i &= T_e \\ K_i \frac{\partial T_i}{\partial z} &= K_e \frac{\partial T_e}{\partial z} \end{aligned}\right\} \qquad z = h_i$$

$$\left.\begin{aligned} T_e &= T_s \\ K_e \frac{\partial T_e}{\partial z} &= K_s \frac{\partial T_s}{\partial z} \end{aligned}\right\} \qquad z = h_i + h_e$$

$$T_s = T_o \qquad z = h_i + h_e + h_s \qquad (2)$$

The solution can be written as:

$$\left(\frac{h_i}{K_i}+\frac{h_e}{K_e}+\frac{h_s}{K_s}\right)(q_o - I_o) = T_f - T_o$$

$$- A_1 I_o \left\{\frac{1-\exp(-\lambda_{s1}h_s)}{K_s\lambda_{s1}} + \frac{\exp(-\lambda_{s1}h_s)[1-\exp(-\lambda_{e1}h_e)]}{K_e\lambda_{e1}} + \frac{\exp(-\lambda_{s1}h_s-\lambda_{e1}h_e)[1-\exp(-\lambda_{i1}h_i)]}{K_i\lambda_{i1}}\right\}$$

$$- A_2 I_o \left\{\frac{1-\exp(-\lambda_{s2}h_s)}{K_s\lambda_{s2}} + \frac{\exp(-\lambda_{s2}h_s)[1-\exp(-\lambda_{e2}h_e)]}{K_e\lambda_{e2}} + \frac{\exp(-\lambda_{s2}h_s-\lambda_{e2}h_e)[1-\exp(-\lambda_{i2}h_i)]}{K_i\lambda_{i2}}\right\}$$

$$+ Q_{si}\, h_s\left(\frac{h_i}{K_i}+\frac{h_e}{K_e}+\frac{h_s}{K_s}\right) - \frac{Q_{si}\, h_s^2}{2\,K_s} \qquad (3)$$

Where the conductive heat flux between the ice-cover and the atmosphere, q_o is defined as:

$$q_o = -K_s \left.\frac{\partial T_s}{\partial z}\right|_{z= h_i + h_e + h_s} \qquad (4)$$

The extension to any number of layers is obvious. As described by Patterson & Hamblin (1988), the thermodynamic balance at the surface depends on the meteorological forcing and on q_o. The surface temperature, T_o, will adjust itself so that a heat flux balance is achieved. T_o, however is bounded by T_m, the melting temperature. This provides the condition for surface melting:

$$q_o(T_o) + H(T_o) = 0, \qquad T_o < T_m$$

$$= -\rho L\frac{dh}{dt}, \qquad T_o = T_m \qquad (5)$$

and, $H(T_o) = R_{li} - R_{lo}(T_o) + Qc(T_o) + Qe(T_o) + Q_r(T_o)$, (6)

where, $H(T_o)$ = net incoming meteorological flux

R_{li} = incoming long-wave radiation

R_{lo} = outgoing long-wave radiation

Q_c = sensible heat transfer between surface and atmosphere

Q_e = evaporative heat flux

Q_r = heat transfer due to rain.

The heat flux in the ice at the ice-water interface, q_f, is obtained from the solution of the heat conduction equation:

$$q_f = -K_i \left.\frac{\partial T_i}{\partial z}\right|_{z=0}$$

$$= q_o - A_1 I_o\{ 1 - \exp[-(\lambda_{s1}h_s+\lambda_{e1}h_e+\lambda_{i1})]\} - A_2 I_o\{ 1 - \exp[-(\lambda_{s1}h_s+\lambda_{e1}h_e+\lambda_{i1})]\} - Q_{si}\, h_s \quad (7)$$

Independently, the heat flux from the water to the ice, q_w, depends only on the conditions in the water column. Any imbalance between q_f and q_w results in the freezing or melting of ice:

$$q_f - q_w = \rho_i L_i \frac{dh_i}{dt} \quad (8)$$

Although melting of either snow, snow-ice or pure ice may occur, only pure ice may be formed at the ice-water interface. The flux of heat from the water to the ice is due only to conduction if the water can be considered stagnant. In this case:

$$q_w = -K_w \left.\frac{dT_w}{dz}\right|_{z=0} \quad (9)$$

where, w = water

Model Description

The formulation given above is the theoretical basis of the model developed herein, MLI (Mixed Lake with Ice cover). Over the winter period, the lake considered here is nearly isothermal, owing to its shallow depth. Hence the internal hydraulics, which can cause rapid changes to thermal structure are ignored and the short sub-daily time steps used in DYRESM are not required. In accordance with lake modeling convention, daily meteorological data are applied to standard bulk aerodynamic formula in order to calculate the average daily meteorological flux at the lake surface. In this case two sub-daily time steps (a day and a night step) are used to resolve the period of solar heating.

The remaining problems which are particular to small mid-latitude lakes are described here, in the context of the MLI model, and with specific reference to the observations made in this study.

Snow Density

In DYRESMI, the snow density is assumed to remain at a constant 330 kg/m^3. Dry falling snow, however, may be as light as 10 kg/m^3, and the presence of liquid water may increase the density of melting snow to as high as 500 kg/m^3 (McKay, 1968). Initially there is rapid settling following a snowfall, with the highest rates of densification occurring within the first few hours following deposition. Here, an exponential decay formula which predicts density as a function of time was developed, based on data gathered from the literature:

$$\rho_s = \rho_n + (\rho_m - \rho_n)(1 - e^{-kd}) \qquad (10)$$

where, $k = -\ln\left(\frac{\rho_m - \rho_1}{\rho_m - \rho_n}\right)$

ρ_n = density of fresh snow

ρ_1 = density of snow 24 hours after falling

ρ_m = maximum density of snow

d = number of days since the last snowfall

The empirical equation given by Grant & Rhea (1973) was specifically considered in choosing an initial density, ρ_n, of 80 kg/m^3 because it is based on observations at an altitude which is comparable to that of the field location chosen for this investigation. The density after 24 hours, ρ_1, was set to 100 kg/m^3, and the maximum density, ρ_m, was set to 200 kg/m^3 for $T_0 < 0$°C, or 300 kg/m^3 for $T_0 > 0$°C. These values produce densities which are consistent with the field observations made during this study. If there are two layers of snow (that is, if there have been two or more snowfalls over the simulation period), then the lower layer is assumed to be at ρ_m, the density of the fresh snow is set to ρ_n, and d is reset to 1.

Snow Conductivity

The thermal conductivity of snow increases substantially with density. Ashton (1986) recommends the following empirical relationship for estimating snow conductivity:

$$K_s = 0.021 + 4.2 \times 10^{-3} \rho_s + 2.2 \times 10^{-9} \rho_s^3 \qquad (11)$$

Snow-Ice Production

In order to determine if flooding of the snow cover will occur, the force balance given in Patterson & Hamblin (1988) must be modified for the case where a snow-ice layer already exits in the cover. The equilibrium depth of snow supported by the ice cover, h_{sm}, is given by:

$$h_{sm} = \frac{h_i (\rho_w - \rho_i) + h_e (\rho_w - \rho_e)}{\rho_s} \qquad (12)$$

If h_{sm} is less than the total snow thickness, h_s, including the most recent snowfall, then flooding will occur. The calculation of the depth of flooding is complicated by the possible existence of two snow layers of different densities. First, equation (12) may be applied using the average snow density to determine if flooding will occur. If so, then the depth of flooding may be calculated in one of two ways depending on the thickness of each snow layer. If two snow layers exist then equation (12) is modified so that the depth of flooding is calculated based on the existence of four mediums. Otherwise, equation (12) is applied as shown to determine the maximum snow thickness which can be supported by the ice. The new snow-ice produced, h_{en}, is equal to the difference between h_s and h_{sm}, and is added to the total snow-ice thickness, h_e. Q_{si}, the sensible and latent heat added to the snow layer by virtue of the flooding, is calculated as follows:

$$Q_{si} = (T_w c_{pw} + L) \rho_w \frac{h_{en}}{h_s} \left[1 - \frac{\rho_s}{\rho_w} \right] \qquad (13)$$

where, Q_{si} = heat generated per unit volume of snow

T_w = water temperature

L = latent heat of fusion

The factor h_{en}/h_s in equation (13) accounts for the fact that, although it is assumed that Q_{si} is uniformly distributed over the new value of h_s, in reality it is only distributed over h_{en}. The $(1-\rho_s/\rho_w)$ term is added to reflect that the water which seeps into the snow layer must be distributed throughout the snow pore structure. Q_{si} is assumed to be distributed over the entire day.

Snow Albedo

In DYRESMI, the albedo is assumed to be constant at 0.85 in sub-zero conditions, and 0.6 during melting conditions. A much wider range, however, has been reported by Grenfell, Perovish & Ogren (1981), Gray (1970), Henderson-Sellers (1984) and others. The work of Strickland (1982) illustrates the need to determine an appropriate albedo on a day by day basis, depending on the environmental conditions. In order to avoid increased field data requirements, empirical relationships relating albedo to meteorological conditions (and not the physical nature of the snow) were sought from the literature. The U.S. Army Corps of Engineers (1956) derived two time dependent decay functions for mountain snowpack albedo predictions. Both express the change in albedo, $\Delta\alpha$, only in terms of the number of days, d, since the last snowfall:

$$\Delta\alpha = \frac{-10^{(0.78-0.69d)}}{100} \qquad \text{(accumulating)}$$

$$\Delta\alpha = \frac{-10^{(1.05-0.07d)}}{100} \qquad \text{(melting)} \qquad (14)$$

Albedo also decreases with increasing solar elevation. This is accounted for using Petzold's (1977) figure 2a, to which the following expression has been fitted:

$$\Delta\alpha = \frac{-1.9 + 24.8\, e^{-\beta/15.5}}{100} \qquad (15)$$

where, β = solar noon angle

Petzold (1977) also performed a regression analysis, using data from four polar stations, to derive a simple relationship expressing the change from clear sky albedo to a value under a given cloud cover:

$$\Delta\alpha = \frac{0.449 + 0.0097 \cdot (10 \cdot C)^3}{100} \qquad (16)$$

where, C = fraction of sky obscured by cloud

Following Petzold (1977), the albedo is initially set to 0.84 as is customary when using the USACE albedo decay functions. This base value is modified in accordance with the sky conditions, equations (15) and (16), to produce α. If no snow has fallen, α_b is modified using the aging functions (14) prior to the sky condition adjustments. In the case of rain, 0.05 is subtracted from α_b provided that it is not already less than 0.8.

Given that the field location chosen for this study is remote and well over 1000 m above sea level, snow purity should be high. The solar angle is also low over much of the simulation period. It would therefore be reasonable to suspect that the albedo was often in excess of 0.9 following snow accumulation events. Although the reduction in albedo in the case of rain is arbitrary, results for the full spectrum of observed conditions are within the appropriate ranges given by Henderson-Sellers (1984) for various surface conditions. Furthermore, a significant reduction in albedo following rain events is justifiable given that an increase in average grain size will result due to fine flake destruction and metamorphosis to granular snow. Both Petzold (1977) and Strickland (1982) attributed lower than predicted albedo observations to rainfall.

Rainfall

Snowmelt due to rain may be an important factor in the depletion of a snowpack. This possibility was ignored in the DYRESMI formulation because it is a rare event at high latitude lakes (Patterson & Hamblin, 1988). When rain falls on snow, the sensible heat associated with

the rain water is given up to the snow. If the heat transferred is more than sufficient to raise the snow temperature to 0°C, then the excess heat results in snowmelt. The heat released to the snow is given as follows:

$$Q_{rs} = C_{pw}\,\rho_w\,(T_{air} - T_m)\,P \qquad (17)$$

where, Q_{rs} = sensible heat released to snow

P = total rainfall

C_{pw} = heat capacity of water

T_{air} = air temperature

It is often assumed that when rain does occur, the snowpack is isothermal at 0°C and all of the heat associated with the rain is used to melt snow (USACE, 1956; Harr, 1981). Harr (1981) uses this assumption in illustrating that rain is only a significant contributor to snowmelt in forested watersheds when total daily rainfall is in the order of several centimetres. If a sub-freezing snow pack were assumed, melt due to rain would be shown to be even less significant. However, in this latter case, the rain water would freeze inside the snowpack, thereby releasing latent heat:

$$Q_{rl} = L\,\rho_w\,P \qquad (18)$$

Although some snow is melted directly by the rain, the associated high humidity and air temperature results in heat transfer to the snow dominated by condensation of water vapour. Condensation will occur in warm, humid conditions when the vapour pressure of the air above the snow exceeds the saturation vapour pressure at the temperature of the snow surface. When precipitation is less than 13 cm/day, condensation is 4 times more important than the sensible heat released from rainfall (Harr, 1981). Condensation is handled by the bulk aerodynamic equations adopted for use in the MLI heat budget.

Both sensible and latent heat derived from rainfall is included in the surface balance (equation 6) in the MLI model. It would likely be more realistic to treat the latent heat as an additional

internal source of heat in the snow cover. The use of daily meteorological averages, however, results in under-estimation of both condensation melt and sensible heat transfer from the rainfall to the snow. Ideally, the average humidity and air temperature associated with the rainfall period would be used in calculating Q_{rs} and Q_e, not the average daily values. Without the latent heat term in the surface balance, the model would incorrectly predict very little snowmelt.

Accretion and Ablation at the Ice-Water Interface

In order to calculate q_w, information regarding the thermal boundary layer at the interface is required. Although detailed measurements are not available, field observations indicate that a linear decrease of temperature from T_w to T_m over a thickness of 0.5 m is a reasonable representation of the thermal gradient at the ice-water interface. The equation for q_w is therefore:

$$q_w = -K_w \left.\frac{\partial T}{\partial z}\right|_{z=0} = -K_w \frac{T_w - T_m}{0.5} \qquad (19)$$

The Link Between Water and Ice

As described earlier, the lakes considered here are small and have large retention times. Therefore, we assume that turbulent heat transfer between water and ice may be neglected and that the temperature is uniform over the water column. Thus, the link between the ice cover and the water below is only due to the term T_w in equation (19). This equation may be evaluated independently, however, using T_w from the previous time step, since the associated change in T_w is small.

Sediment Heat Transfer

Observed sediment heat transfer rates at both mid and high latitude lakes during ice-covered periods are typically in the range of 1 to 5 W/m^2 (see Ashton, 1986; Birge et al, 1927; Likens & Johnson, 1969; Welch and Bergmann, 1985; Mortimer & Mackereth, 1958). Falkenmark

(Ashton, 1986) derived an empirical formula relating the sediment heat budget to mean depth only. It is preferable, however, to base estimates on the heat conduction equation. Unfortunately, no quantitative data are available regarding the conductivity or the thermal gradients in the sediments of the lake observed in this investigation. Rough estimates however, may obtained using an average conductivity from previous investigations, and information regarding the lake heat budget. Assuming a linear increase in temperature from the average annual whole lake temperature to the actual lake temperature over a sediment thickness, z_{sed}, the thermal gradient at the sediment-water interface may be calculated as:

$$\frac{dT}{dz} \approx \frac{T_y - T_w}{z_{sed}} \tag{20}$$

where, T_y = the average annual whole lake temperature

T_w = the current water temperature

z_{sed} = distance over which sediment temperature (linearly) increases from T_y to T_w

= 2 meters, based on the observation that temperatures below 2 m remain more or less constant over time (Ashton, 1986).

From the literature, an average conductivity of 1.2 W/m^{o}C produces a heat transfer rate of about 2.8 W/m^2 at the lake chosen for this study, if an average T_w of 3^{o}C for the winter period is assumed.

A summary of the values chosen for the parameters required for MLI are given in Table 1. With regard to solar attenuation, in spite of few data, it is clear from the literature (see Grenfell & Maykut, 1977) that λ_e should lie between λ_i and λ_s. The average of λ_s and λ_i as given by Patterson & Hamblin (1988) was selected as an appropriate first estimate of λ_e. Similarly, the conductivity of snow-ice should lie in between that of snow and that of ice. Since the voids in the snow are filled with water and subsequently frozen, it is reasonable to expect K_e to be closer to K_i than K_s. A value of 2.0 W/m^{o}C was selected.

Table 1 Summary of Parameters

Parameter	Value	Parameter	Value
λ_{i1}	1.50 m^{-1}	ρ_i	917 kg/m^3
λ_{s1}	6.00 m^{-1}	ρ_e	890 kg/m^3
λ_{e1}	3.75 m^{-1}	ρ_s	Equation 10
λ_{i2}	20 m^{-1}	α_s	variable
λ_{s2}	20 m^{-1}	α_i	0.02
λ_{e2}	20 m^{-1}	α_{si}	0.45
K_s	Equation 11	α_w	0.06
K_i	2.3 W/m/°C	ρ_n	80 kg/m^3
K_e	2.0 W/m/°C	ρ_1	100 kg/m^3
K_{sed}	1.2 W/m/°C	ρ_m	200 - 300 kg/m^3

Field Study Description

The model described above was applied to Harmon Lake, which is located in British Columbia's Southern Interior Plateau, about 300 km north-east of Vancouver, and 15 km south-east of Merritt (figure 1). It is a small, naturally eutrophic lake which experiences significant rates of oxygen depletion below the thermocline in summer and under ice-cover in winter. Harmon Lake is the centerpiece of a small provincial park and is very popular among recreational anglers. A bathymetric map of Harmon Lake is shown in figure 2.

In order to utilize and verify MLI, a significant effort was required to acquire field data. Meteorological data were collected from a weather station installed in mid-December, 1991 at Menzies Lake, approximately 5 km from and 100 m higher in elevation than Harmon Lake. As the model was designed for future compatibility with DYRESM, the input requirements are similar. The bulk aerodynamic equations suggested by the TVA (1972) and employed in MLI require the following meteorological data:

a) air temperature

b) wind speed

c) total daily solar radiation

d) humidity

e) cloud cover

f) precipitation

No direct means was available of sensing cloud cover, but an empirical relationship exists which expresses cloud cover in terms of the observed and theoretical clear-sky solar radiation (TVA, 1972; see Rogers, 1992). The remaining meteorological variables are plotted in figure 3. Local assistance was available to measure snow depth using snow boards and a metre stick, and to ensure that the solar radiation sensor remained clear of snow. Given that rainfall at the field location is rare over the winter months, no means for measuring rainfall was provided. (Less than 2 cm in total fall, on average, from December to March in the Southern Interior Plateau. Even less is expected at the field location due to its high elevation.) The local resident noted all days on which rainfall occurred. For these days, the rainfall data from the city of Merritt, 500 m lower in elevation and about 20 km to the North, was used for snowmelt predictions. Although rainfall was observed at Merritt on every day that it was noted at the lake, there was no significant correlation between the precipitation measurements at Menzies Lake and those at Merritt ($r = 0.37$). Therefore, no adjustments to the Merritt rainfall data could be justified for use in the MLI model.

Snow depth, ice thickness, and lake temperature were measured during field trips to the lake, which took place about once every two weeks. Temperatures were measured at one metre intervals at the location of maximum depth.

Simulation Results

The model described above was written in QUICKBASIC 5.0 and run in 32 bit precision on an 80386 DX (25 MHz) PC equipped with an 80387 math co-processor. An important feature of

MLI is the reduced computational requirement compared with DYRESMI, due to the neglect of internal thermodynamics. For the 105 day-long simulation described here less than 10 seconds of central processor time were required to produce the results.

The results produced by MLI for Harmon Lake using the default parameters given in Table 1 are shown in figure 4. Given the approximations made in the development of the model, the results are very good. The estimated errors in the observations account for most of the difference between the observed and predicted variables. Rogers (1992) found that reasonable variations in some of the default parameters provide an improved fit to the observations. Results from sensitivity analyses indicate that the following parameter changes may be appropriate: an increase in K_s and λ_e, and a decrease in sediment conductivity and albedo during melting conditions (Rogers, 1992). No conclusive evidence, however, is available to justify any particular parameter changes.

The trends in temperature and ice and snow thicknesses are generally well predicted by the model. The results, however, suggest that some problems remain unsolved. Difficulties include snow compaction, as illustrated by the underprediction of snow thickness in early January and solar attenuation, as indicated by the unlikely surge in temperature in mid-February. The model does, however, continue to provide good predictions even in late March when an ice-zone 1 to 4 metres in width around the perimeter of Harmon Lake was observed. This observation emphasizes the fact that, although assumed to be uniform, the ice thickness can be highly variable over the lake surface.

Results using the DYRESMI formulation are also given in figure 4. The MLI model provides an improved prediction of a mid-latitude lake winter heat budget over DYRESMI. Considering the latter model first, the initial predicted total ice and snow thicknesses do not match with observations because the initial ice thickness could not support the weight of the observed snow (figure 4). This is explained by the high snow density assumed to be appropriate for the lakes considered by Patterson & Hamblin (1988). Hence DYRESMI predicts instant flooding of the

ice cover from the initial conditions. Furthermore, DYRESMI predicts ice thicknesses almost 50% greater than the observations throughout most of the modeling period. This is primarily due to the relatively high snow conductivity associated with the assumed density. Using equation (11) and the range of densities assumed in this study, MLI predicts snow conductivities of about 20% to 60% of the constant value of 0.31 W/m°C assumed in DYRESMI.

In addition, DYRESMI generally over-predicts the snow thickness for two principal reasons. First, it is assumed that no settling or wind transport of snow occurs, and secondly, rain melt is ignored. Some surface melt is predicted by DYRESMI at the end of January, when most of the rain fell, because the meteorological flux balance produces a surface temperature of 0°C on several consecutive days. Neglect of heat released to the snow cover due to flooding may also contribute to the inadequate snowmelt predicted by DYRESMI.

Turning to lake temperature, DYRESMI predicts cooling over the first two months of the simulation because of the neglect of sediment heat transfer. Less solar heating is also predicted during some periods when over-prediction of snow and ice thicknesses occur. DYRESMI also under-predicts the rapid increase in lake temperature in March. This can only be explained by an under-prediction of solar penetration. There are two major factors which lead to this result. First, MLI, on average, predicts a lower albedo than DYRESMI over the latter period of the simulation. Secondly, there is high solar attenuation due to the over-prediction of snow and ice thicknesses.

The Surface Heat Balance

The components of the surface heat budget and the direct heat fluxes to and from the lake water are shown in figure 5. The meteorological balance results in a net loss of heat from the lake surface over the first half of the simulation, facilitating a period of sustained ice growth. Most important in the early winter balance is a net emittance of long-wave radiation. The evaporative flux is generally negligible over the entire modeling period. The sensible heat transfer almost

always constitutes a source of heat to the lake surface, not a sink. This latter result is due to the fact that the solution to the conduction equation yields surface temperatures, T_o, which are consistently below air temperatures, T_{air}. Both Ashton (1986) and the U.S. Army Corps of Engineers (1956) provide thermal profile measurements across the air-snow interface which are consistent with these results. No examples were found in the literature where $T_o > T_{air}$ for a snow covered surface.

Although there is, on average, an increase in the net emittance of long-wave radiation towards the end of the simulation period, both solar radiation and sensible heat transfer increase substantially. This results in a reverse in the flux imbalance at the ice-water interface thereby causing the ice to melt.

Although most of the transmitted solar radiation is absorbed in the cover (about 90% in December, decreasing to about 75% in March), the heat is distributed throughout the cover, albeit not uniformly, thereby diminishing the tendency to counter the heat flux out of the lake. Therefore, when solar radiation appears to tip the balance in favour of a net gain of heat in early February, there is actually a continued period of heat loss and ice formation until well into the latter half of the month.

It can be seen from figure 5 that the heat due to rainfall is in most instances, sufficient when combined with high rates of sensible heat transfer into the lake to reverse the direction of the surface heat flux, and cause surface melting. Since almost all of the heat generated by the rainfall is assumed to be latent heat, there would not be sufficient melt predicted if this heat were not included in the surface meteorological balance. According to Harr (1981), there should have been significant amounts of heat derived from condensation (as quantified by Q_e) to produce surface melt. The warm temperatures and high humidity which likely persisted over the rainfall periods are not reflected in the daily averages.

Results also indicate that the rate of ice melt in March is also under-predicted. Several explanations are available. The difficulty of accurately predicting the presence (or absence) of very thin layers of snow, which may have a huge effect on the albedo, is recognized. The open ice area around the perimeter of the lake which developed in March probably served to encourage convective circulation in the lake, resulting in an increased transfer of heat from the water to the ice. It is probable that this last mechanism was most important in increasing ice melt since it does not necessarily involve an increase in lake temperature, the trend of which is quite well predicted over the last month of the simulation. An addition, the average albedo may have been significantly decreased due to heavy snowmobile traffic on the lake. The observed impact included local compaction and snow melt in addition to ponding in the tracks created by the snowmobiles.

The heat produced by ice cover flooding is substantial. Several snowfalls occur in mid-January which exceed the bearing capacity of the ice cover. Sensitivity analysis has indicated that the flooding causes a significant reversal in the balance between q_f and q_w, which translates into substantial melting at the ice-water interface (Rogers, 1992). The primary source of this heat is the latent heat of fusion resulting from the formation of snow-ice. The net effect of this process, however, is an increase in the total ice thickness due to the accumulation of snow-ice. In fact, the net rate of growth is substantially higher over the period of these snowfalls than over the preceding month.

The heat fluxes to and from the unfrozen lake are also shown in figure 5. Although solar radiation is responsible for almost all of the heat absorbed by the lake water over the modeling period, predicted sediment heat transfer rates exceeded the rate of solar heating in early winter. By February, however, solar heating dominates strongly as the sediment heat transfer begins to fall in response to a reduced thermal gradient.

Over most of the period, sediment heating is only slightly more than offset by heat conduction through the ice. The gap widens, however, starting in February, as the lake begins to heat up

more rapidly. By the end of the simulation period, conduction through the ice cover is more than four times the diminishing sediment heat transfer rate. At this time, however, conduction of heat to the ice is only 5 to 10% of the daytime averages of solar heating.

Conclusions

It has been found that solar heating is the main cause of lake warming over the ice-covered period but, unlike deep lakes, sediment heat transfer may at least counter conductive heat loss to the ice cover to prevent a reduction in temperature in early winter. In addition, rain events may lead to a significant increase in lake warming due to reduced albedo. Ice thicknesses may be reduced as a result of the heat associated with rain, but it may eventually cause an increase in ice thickness if the insulation provided by the snow cover is lost and cold conditions follow. The impact of snow-ice formation is similar in that mass is added to the total ice thickness, but the associated latent heat may result in melting at the ice-water interface.

MLI is superior to DYRESMI in terms of mid-latitude lake simulation. Poor predictions by DYRESMI result primarily from the use of inappropriate parameters such as snow density, thermal conductivity and albedo, which clearly must be considered as variables for mid-latitude lake applications. Furthermore, the neglect of rain melt, and, to a lesser degree, the heat associated with snow-ice production, leads to over-predictions of snow thickness, and under-predictions of lake heating.

It is clear that the water which floods the snowpack when the bearing capacity of ice is exceeded constitutes a source of heat within the cover. This heat, however, as represented by Q_{si}, may be over-estimated, since further snow densification likely occurs prior to the snow-ice formation. In addition, capillary rise may contribute to the snow-ice thickness.

The latent heat associated with rainfall was needed to produce the order of observed surface melting. Although the results are reasonable, the mechanism is unlikely. As described earlier, condensation melt should be the main driving force behind snowmelt for the given amounts of

precipitation. It is suspected that the use of daily average meteorological data leads to an under-representation of condensation melt. It is therefore concluded that a purely theoretical representation of snowmelt due to rain will not produce accurate results unless sub-daily averages of meteorological data are used.

Accurate prediction of snowmelt is essential, especially when the snow cover is thin. Even slight inaccuracies may lead to much more significant inaccuracies in ice and temperature predictions because of the significant drop in albedo (and to a lesser extent, the increase in conduction) associated with ice exposure when the snow is completely melted. This explains the unlikely surge in lake temperature due to solar heating following the incorrect prediction of complete snowmelt in mid-February.

The correct combination of parameter values which would provide more accurate predictions is not completely evident from this study. Much work is required to quantify narrow ranges of possible values for mid-latitude locations. The relationships between snow density, conductivity, solar attenuation and albedo are of the greatest importance. A physically based model of snow densification is also needed.

Further research should concentrate on the properties of the ice and snow cover, and the lake sediments. This would involve including direct measurements of snow density, conductivity, solar attenuation, albedo, and sediment conductivity, in addition to repeating the data collection and modeling process. In order to show that there are no other parameters of importance to the results, additional steps will be required to prove the accuracy of the model. These include a better understanding of the heat fluxes due to rainfall and snow-ice formation, and at the sediment-water and ice-water interfaces.

List of Symbols

A .....spectral fraction

C.....fraction of sky which is cloud-covered

C_{pi} .....heat capacity of ice

C_{pw}.....heat capacity of water

d .....number of days since snowfall

H .....net meteorological flux

h .....thickness of medium

h_{en} .....latest snow-ice accumulation

h_{sm} .....maximum possible snow thickness

I_o .....non-reflected solar radiation at surface

K.....conductivity

L.....latent heat of fusion

P .....rainfall

q_f .....heat flux in ice at ice-water interface

q_o.....heat flux at the surface

Q_{sed}.....sediment heat flux

q_w .....heat conduction from water to ice

Q_c.....sensible heat flux

Q_e.....evaporative heat flux

Q_o.....incoming solar radiation

Q_r .....heat due to rainfall

Q_{si} .....heat due to snow-ice formation

R_{li}.....incoming long-wave radiation

R_{lo} .....outgoing long-wave radiation

T.....temperature

z.....vertical coordinate (depth)

Subscripts

1 .....visible spectrum of radiation

2 .....infrared spectrum of radiation

e.....snow-ice

f.....freezing

i .....ice

m .....melting

o .....surface

s .....snow

sed.....sediment

w .....water

Greek Symbols

α.....albedo

β .....solar angle at solar noon

λ .....solar attenuation coefficient

ρ .....density

ρ_1 .....snow density 24 hours after snowfall

ρ_m .....maximum snow density

ρ_n .....density of new snow

REFERENCES

Ashton, G.D., 1986, ed., River and Lake Ice Engineering, Water Resources Publications, Colorado.

Birge, E.A., Juday, C., March, H.W., 1927, The Temperature of the Bottom Deposits of Lake Mendota: a Chapter in the Heat Exchanges of the Lake, Trans. Wisc. Acad. Sci. Arts Lett. 23, pp. 187-231.

Boer, K.W., 1980, The Terrestrial Solar Spectrum, Solar Energy Technology Handbook, Part A (W.C. Dickenson & P.N. Cheremisinoff [eds.]), Dekker, pp. 65-87.

Chen, C.W., Orlob, G.T., 1975, Ecological Simulation for Aquatic Environments, System Analysis and Simulations in Ecology, B. Patton, ed., Vol. 3, Academic Press, New York.

Gosink, J.P., 1987, Northern Lake and Reservoir Modeling, Cold Regions Science and Technology, no. 13, pp. 281-300.

Grant, L.O., Rhea, J.O., 1973, Elevation and Meteorological Controls on the Density of New Snow, Advanced Concepts and Techniques in the Study of Snow & Ice Resources, U.S. Committee of the International Hydrological Decade, pp. 169-181.

Gray, D.M., 1970, Handbook on the Principles of Hydrology, Canadian National Committee for Hydrological Decade, Ottawa.

Grenfell, T.C., Maykut G.A., 1977, Optical Properties of Ice and Snow in the Arctic Basin, Journal of Glaciology, 18, pp. 445-463.

Grenfell, T.C., Perovich, D.K., Ogren, J.A., 1981, Spectral Albedos of an Alpine Snowpack, Cold Regions Science and Technology 4(2), pp. 121-127.

Harr, R.D., 1981, Some Characteristics and Consequences of Snowmelt During Rainfall in Western Oregon, Journal of Hydrology (53), pp. 277-304.

Henderson-Sellers, B., 1984, Engineering Limnology, Pitman Publishing Ltd., 356 pp.

Imberger, J., & Patterson, J.C., 1981, A Dynamic Reservoir Simulation Model -DYRESM:5, in Transport Models for Inland & Coastal Waters: Proceedings of a symposium on Predictive Ability (H.B. Fischer, ed.), Academic Press, New York.

Kirk, J.T.O., 1983, light and Photosynthesis in Aquatic Systems, Cambridge.

Likens, G.E., Johnson, N.M., 1969, Measurement and Analysis of the Annual Heat Budget for the Sediments in Two Wisconsin Lakes, Limnology & Oceanography, 114(1), pp. 115-135.

Maykut, G.N., Untersteiner, N., 1971, Some Results from a Time Dependent, Thermodynamic Model of Sea Ice, J. Geophys. Res. (83), pp. 1550-1575.

McKay, G.A., 1968, Problems of Measuring and Evaluating Snowcover, Snow Hydrology: Proceedings of the Canadian National Committee of the International Hydrological Decade

Mortimer, C.H., and Mackareth, 1958, Convection and its Consequences in Ice-covered Lakes, Verh. internat. Ver. Limnol., pp. 923-932.

Patterson J.C., & Hamblin, P.F., 1988, Thermal Simulation of Lakes with Winter Ice Cover, Limnol. Oceanogr. 33(3): 328-338.

Petzold, D.E., 1977. An Estimation Technique for Snow Surface Albedo, Climatological Bulletin, McGill University, Dept. of Geography, 21, pp.1-11.

Raphael, J.M., 1962, Predictions of Temperature in Rivers and Reservoirs, Journal of the Power Division, A.S.C.E., 88(PO2), Proc. paper 3200, pp. 157-182.

Rogers, C.K., 1992, Impact of an Artificial Circulation Device on the Heat Budget of an Ice-Covered Mid-Latitude Lake, M.A.Sc. Thesis, The University of British Columbia, 174 pp.

Strickland, N., 1982, Factors Affecting Temporal Variations in the Albedo of Snow Cover, Western Snow Conference, Proceedings, pp. 186-187.

Tennessee Valley Authority (TVA), 1972, Heat and Mass Transfer Between a Water Surface and the Atmosphere, Division of Water Control Planning, Report No. 0-6803, Water Resources Research Laboratory Report No. 14, Norris, Tennessee.

United States Army Corps of Engineers (U.S.A.C.E.), 1956 , Snow Hydrology, Summary Report of the Snow Investigations, North Pacific Division, Portland, Oregon, 437 pp.

Welch, H. E., and Bergmann, M.., 1985, Water Circulation in Small Arctic Lakes in Winter, Can. J. Fish. Aquat. Sci. 42, pp. 506-520.

List of Figures

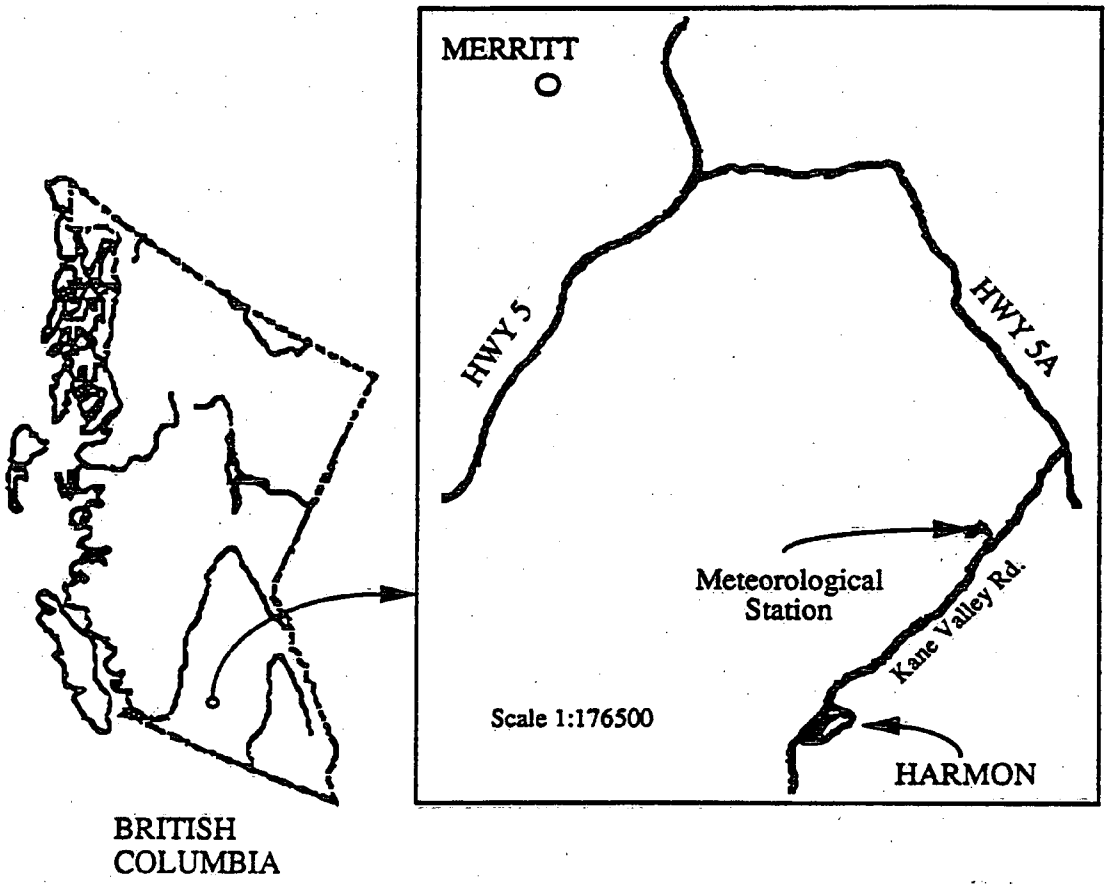

Figure 1 Field Study Location

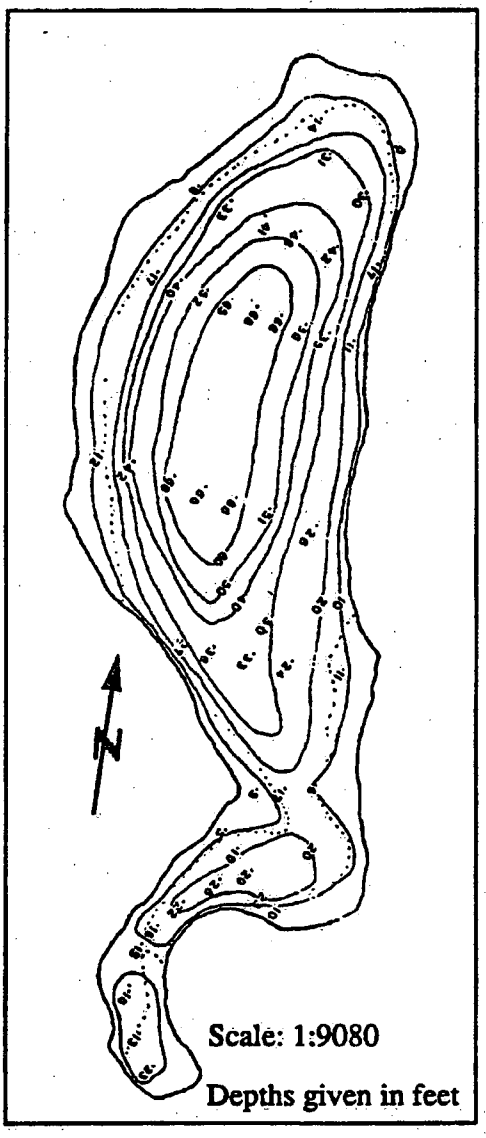

Figure 2 Harmon Lake Bathymetry

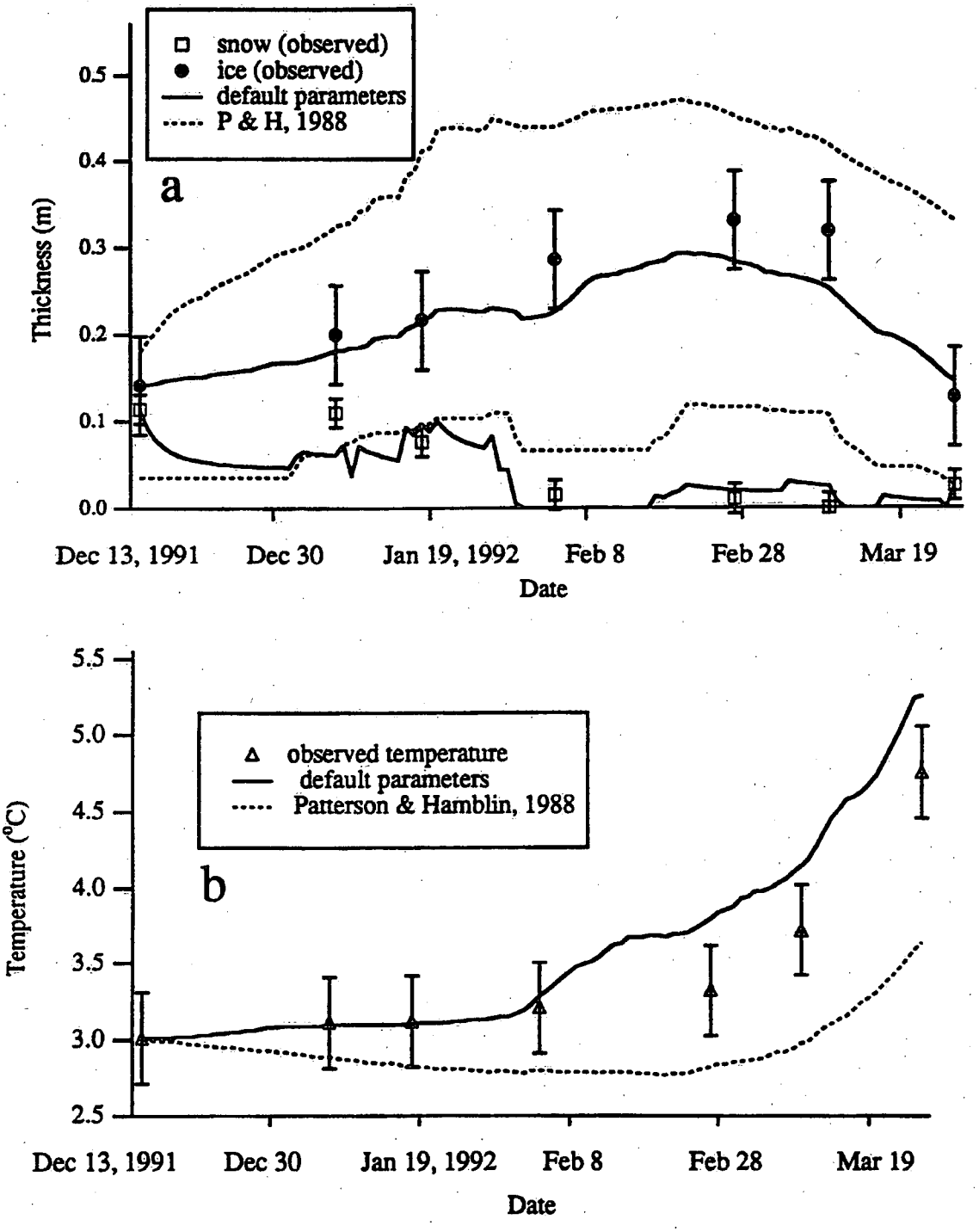

Figure 4 A Comparison of Results for Harmon Lake Using MLI and Patterson & Hamblin's (1988) Model
a) Snow & Ice Predictions
b) Whole Lake Temperature Predictions

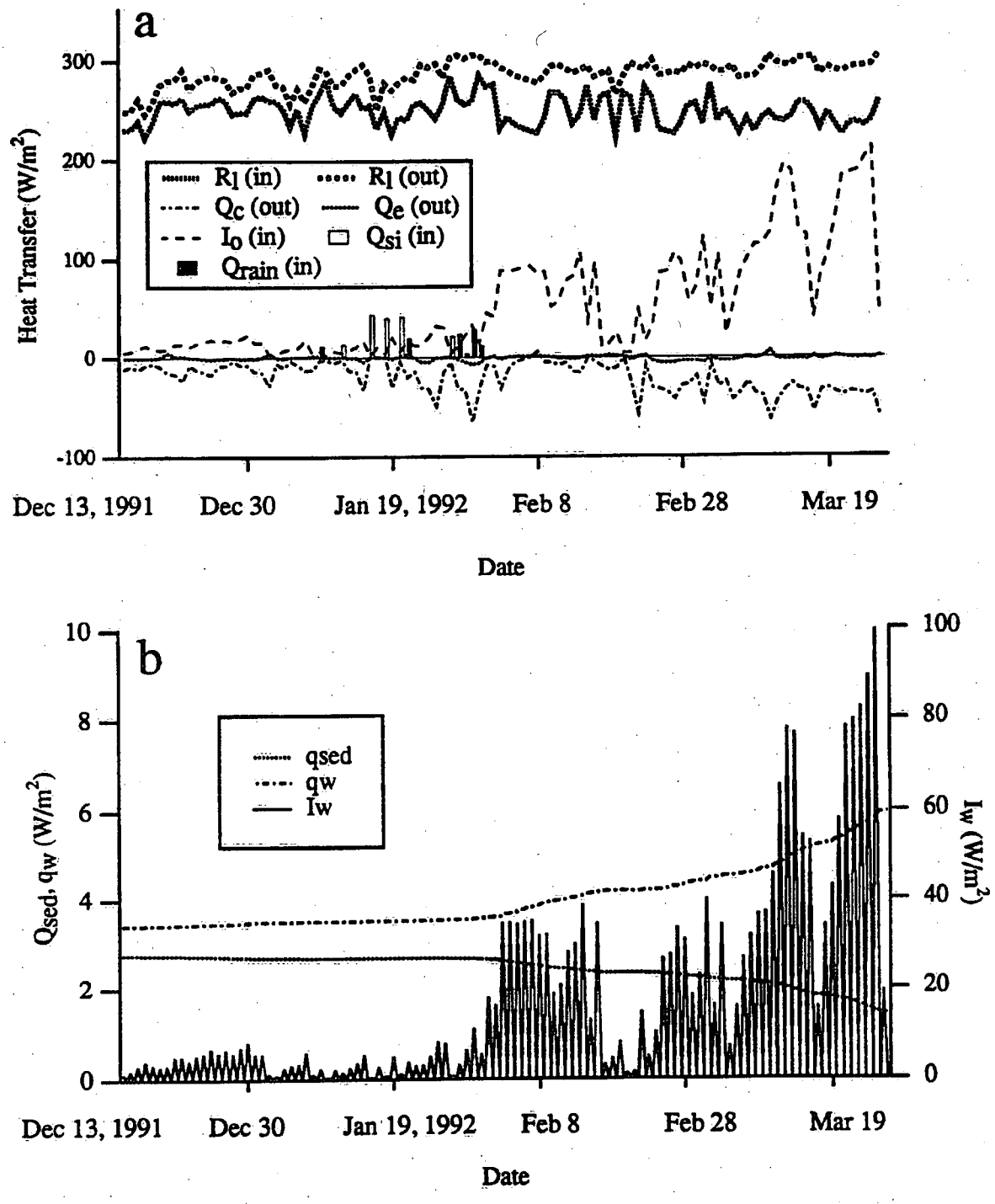

Figure 5 a) Surface Heat Budget Components
b) Heat Fluxes to and from Lake Water
(left hand axis: Q_{sed}, q_w; right hand axis: I_w)

Environment Canada Environnement Canada

Canada

Canada Centre for Inland Waters
P.O. Box 5050
867 Lakeshore Road
Burlington, Ontario
L7R 4A6 Canada

National Hydrology Research Centre
11 Innovation Boulevard
Saskatoon, Saskatchewan
S7N 3H5 Canada

St. Lawrence Centre
105 McGill Street
Montreal, Quebec
H2Y 2E7 Canada

Place Vincent Massey
351 St. Joseph Boulevard
Gatineau, Quebec
K1A 0H3 Canada

Centre canadien des eaux intérieures
Case postale 5050
867, chemin Lakeshore
Burlington (Ontario)
L7R 4A6 Canada

Centre national de recherche en hydrologie
11, boul. Innovation
Saskatoon (Saskatchewan)
S7N 3H5 Canada

Centre Saint-Laurent
105, rue McGill
Montréal (Québec)
H2Y 2E7 Canada

Place Vincent-Massey
351 boul. St-Joseph
Gatineau (Québec)
K1A 0H3 Canada